



Phase Constituent and Microhardness of As-Cast and Long-Time Annealed $\text{Al}_x\text{Co}_{2-x}\text{CrFeNi}$ Multicomponent Alloys

Ya Sun¹ · Changjun Wu^{1,2} · Haoping Peng¹ · Ya Liu^{1,2} · Jianhua Wang^{1,2} · Xuping Su^{1,3}

Submitted: 9 April 2019 / in revised form: 19 September 2019 / Published online: 3 October 2019
© ASM International 2019

Abstract The phase constituent and microstructure of arc-melted $\text{Al}_x\text{Co}_{2-x}\text{CrFeNi}$ multicomponent alloys, in both the as-cast state and after annealed at 800 or 1000 °C for 30 days, were experimentally investigated by scanning electron microscopy and x-ray diffraction. Different phase constituents were obtained in these alloys. The $\text{Al}_{0.25}\text{Co}_{1.75}\text{CrFeNi}$ alloy was composed of a single FCC phase in both as-cast and 1000 °C annealed states. Small amount of B2 phase precipitated after 800 °C annealing. A eutectic structure was observed in the $\text{Al}_{0.75}\text{Co}_{1.25}\text{CrFeNi}$ alloy. Its morphology kept, but small amount of σ phase separated, after being annealed at 800 °C for 30 days. In the $\text{Al}_x\text{Co}_{2-x}\text{CrFeNi}$ ($x = 1.25\text{--}1.75$) alloys, a single B2 phase was obtained in the as-cast state, it would turn to two-phase of BCC + B2 after 800 °C or 1000 °C annealing. The as-cast AlCoCrFeNi alloy was also composed of a single B2 phase, it would transform to four phases of BCC + B2 + FCC + σ after 800 °C annealing, and to two phases of B2 + FCC after 1000 °C annealing for the σ phase is not stable at 1000 °C. Moreover, experimental results

indicated that the alloy hardness increased with the Al content. The existence of the σ phase could obviously harden the alloy. Except for the alloys with σ precipitation, the hardness of the annealed alloys was lower than that of the as-cast ones. In addition, increasing the annealing temperature coarsened the grains and softened the alloys.

Keywords Al-Co-Cr-Fe-Ni · annealing · microstructure · multicomponent alloys

1 Introduction

High-entropy or multicomponent alloys,^[1–4] which have at least five major metallic elements with the atomic fraction of each principal element being between 5 and 35% (all compositions herein are in at.% unless otherwise specified), are different from conventional alloys. Recently, these alloys have been widely researched. Because the CoCrFeNi alloy is a single FCC phase with high tensile ductility and fracture toughness,^[5] most researchers added one or two elements into equiatomic CoCrFeNi alloys for strengthening.^[6–12] Among these systems, the Al-Co-Cr-Fe-Ni multicomponent alloys have been widely studied for their extremely high strength, excellent thermal stability and corrosion resistance.^[13–18] In Al-Co-Cr-Fe-Ni multicomponent alloys, Fe and Co tend to segregate to the dendrites, while Al and Cr segregate to interdendrites.^[19] Furthermore, Al can stabilise the BCC phase^[1,2] and Co is an FCC stabiliser.^[20] Nevertheless, too much attention has been paid to the pseudo-binary Al-CoCrFeNi ,^[16,21–29] limiting the diversity of Al-Co-Cr-Fe-Ni multicomponent alloys.

✉ Changjun Wu
wucj@cczu.edu.cn

¹ Jiangsu Key Laboratory of Materials Surface Science and Technology, Changzhou University, Changzhou 213164, People's Republic of China

² National Experimental Teaching Demonstration Center of Materials Science and Engineering, School of Materials Science and Engineering, Changzhou University, Changzhou 213164, People's Republic of China

³ Jiangsu Collaborative Innovation Center of Photovoltaic Science and Engineering, Changzhou University, Changzhou 213164, People's Republic of China

Heat treatment is a common method to acquire nanostructures and stabilise the phases.^[30] $\text{Al}_{0.3}\text{CoCrFeNi}$ alloys have higher tensile strength and ductility at ambient temperature than at cryogenic temperature.^[31] Niu et al.^[32] studied an $\text{Al}_{0.5}\text{CoCrFeNi}$ alloy annealed at 650 °C for 0.5–8 h and reported that the heat treated alloy had a superior combination of strength and plasticity. In addition, for potential application in high heat areas, the phase stabilities of high-entropy alloys at high temperatures need to be understood. Butler and Weaver^[33] reported that the microstructure of $\text{Al}_x\text{CoCrFeNi}$ ($x = 0.5\text{--}1.0$) alloys became coarser after annealing at 1050 °C for 520 h and the alloys consisted of FCC, B2, BCC and/or σ phases after annealing at 700 °C for 1000 h. Tsai et al.^[34] proved that the $\text{Al}_{0.5}\text{CoCrCuFeNi}$ alloy obtained outstanding mechanical properties after annealing. Furthermore, Wu et al.^[35] showed that annealing treatments had a significant effect on the microstructure and properties. Compared with the as-cast alloys, the compression strength increased after annealing.

In spite of intensive investigations in the past few years, the phase stability at high temperature within this multi-component alloy system is still poorly understood and needs to be clarified, which poses obstacles for promising Al-Co-Cr-Fe-Ni multicomponent alloys. Although there are many researches about the $\text{Al}_x\text{CoCrFeNi}$ alloys, the investigation on the $\text{Al}_x\text{Co}_{2-x}\text{CrFeNi}$ alloys is missing. For further understanding of the Al-Co-Cr-Fe-Ni multicomponent alloys and the effect of Al and Co content on their phase constituent, in the present work, the Cr, Fe and Ni contents were fixed at 20 at.%, and a series of $\text{Al}_x\text{Co}_{2-x}\text{CrFeNi}$ alloys were designed and annealed at 800 and 1000 °C for 30 days. The effect of the Al and Co contents and annealing temperatures on the phase constituent, microstructure and microhardness of the alloys were investigated.

2 Experimental

To study the effect of Al and Co contents on the microstructure and microhardness of Al-Co-Cr-Fe-Ni alloys, the Cr, Fe and Ni contents were fixed at 20%, seven $\text{Al}_x\text{Co}_{2-x}\text{CrFeNi}$ ($x = 0.25\text{--}1.75$) alloys were designed. The designed alloys with a total mass of 10 g, consisting of four high-purity components (> 99.95%), were prepared by an arc melting casting method in an atmosphere of purified argon. It is necessary to repeat the melting at least four times to ensure the chemical homogeneity of the alloy. These alloy specimens were then cut into three pieces: one part was used as the as-cast state, while the others were sealed in an evacuated quartz tube and then annealed at 800 and 1000 °C for 30 days, respectively, and quenched in

cold water at the end of the treatment. To differentiate from the as-cast alloys, the 800 and 1000 °C annealed alloys were denoted as A' and A'', respectively.

To conduct the observation of microstructures, the specimens were ground using silicon carbide papers with #400–#2000 grit, and finally, a 1 μm diamond suspension was used to perform surface polishing. The specimens without etching were examined using a JSM-6510 scanning electron microscope (SEM) equipped with an Oxford INCA energy dispersive spectrometer (EDS). The structure of the cylindrical alloys was characterised by x-ray diffraction (XRD) using a D/max 2500 PC x-ray diffractometer with Cu K_α radiation and a 2θ step size of 0.02°. Hardness measurements were conducted using a Vickers hardness tester (HXD-1000TMC/LC) under a load of 200 gf maintained for 20 s.

3 Results

3.1 As-Cast Microstructure

The XRD patterns and back-scattered electron (BSE) images of the as-cast $\text{Al}_x\text{Co}_{2-x}\text{CrFeNi}$ ($x = 0.25\text{--}1.75$) alloys are shown in Fig. 1 and 2, respectively. The SEM-EDS analysis results of each phase or region are listed in Table 1. It is clear that, except for alloys A2 and A3, the others show just single phase. They should be the BCC-type or FCC-type phases according to the XRD patterns in Fig. 1. Based on available information about the Co-Cr-Fe-Ni system,^[5,36] the FCC-type phase in the present work

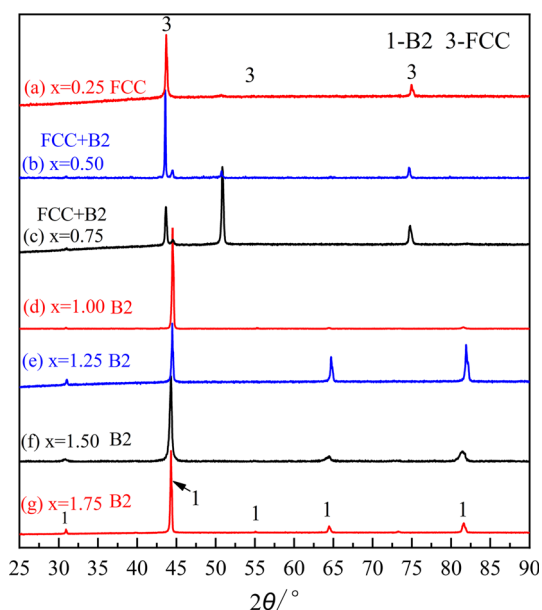


Fig. 1 XRD patterns of as-cast $\text{Al}_x\text{Co}_{2-x}\text{CrFeNi}$ ($x = 0.25\text{--}1.75$) alloys

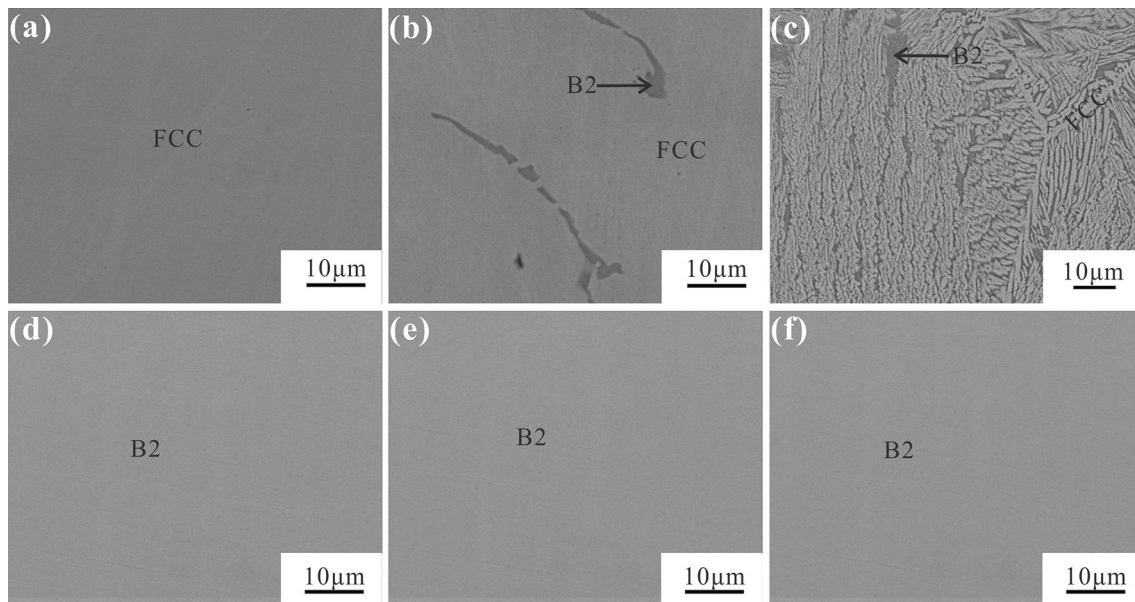


Fig. 2 BSE micrographs of as-cast $\text{Al}_x\text{Co}_{2-x}\text{CrFeNi}$ alloys: (a) A1, $x = 0.25$; (b) A2, $x = 0.50$; (c) A3, $x = 0.75$; (d) A4, $x = 1.00$; (e) A5, $x = 1.25$; (f) A7, $x = 1.75$

should be the FCC solid solution, although it contains less than 10.2 at.%Al. Moreover, according to the thermodynamic calculation based on TCFE database, the FCC solid solution is also stable at 1000 °C for the composition detected in alloy A1. It needs to note that the TCFE database is a Fe-based thermodynamic database and it can not work for the alloy with high Al content. The B2 phase denoted in the present work is judged by its XRD pattern, EDS result and BSE image. Firstly, in the XRD pattern, a small characteristic peak for (100) plane at $\sim 30.9^\circ$ (2θ) is a difference between the BCC solid solution and the ordered B2 phase. Secondly, in the sub-binary systems of the Al-Co-Cr-Fe-Ni system, the ordered B2 phase just exist in the Al-contained binary systems, such as Al-Fe, Al-Ni, Al-Co. And the BCC solid solution is unstable when Al content is above 20 at.%, may because Al has much larger atomic size larger than Co, Cr, Fe, Ni. Moreover, Lim et al.^[37] had also distinguished BCC-A2 and BCC-B2 by selected area diffraction pattern in AlCoCrFeNi alloy. Besides, the B2 phase should be an Al-rich phase and is much darker than BCC phase in BSE image.

The BSE image (Fig. 2a) and XRD pattern (Fig. 1a) show that a FCC single phase exists in the as-cast alloy A1 (5Al135Co20Fe20Cr20Ni). The characteristic peaks of the FCC phase become weak with the increase of the Al content, and the alloy microstructures also change obviously. When the Al content increases to 10% in alloy A2, a darker Al-rich phase appears (Fig. 2b). A weak BCC-type characteristic peak at 44.5° (2θ) is observed in its XRD pattern (Fig. 1b). Actually, there is a very small peak at 30.9° (2θ) which proves the phase is BCC-B2. Moreover,

EDS result shows the darker phase contains 25.5 at.%Al, which is much higher than the Al content in the alloy, as shown in Table 2. With the increase of the Al content, the B2 phase increases. The XRD pattern in Fig. 1c indicates that the FCC and B2 phases coexist in alloy A3. As can be seen from Fig. 2c, a eutectic structure exists in the as-cast alloy A3, which is different from other alloys. In the solidified FCC grains of alloy A3 (Fig. 2c), a significant number of long stripes are formed and it exhibits a dendritic structure. Based on the detected composition, the white phase is the FCC phase while the grey one is the B2 phase with a higher Al content.

The microstructures of alloys A4-A7 are the same and show a single phase. For there are small peaks at $\sim 31^\circ$ (2θ) in their XRD patterns and the Al content is above 19.3 at.%, the single phase in all these alloys were identified by B2 phase. In alloy A4, the characteristic peak at around 44.3° (2θ) is too strong, it takes careful observation to see the peaks at 30.9° (2θ). In these alloys, the Al content increases from 20 to 35 at.%. Based on these results, it is believed that the single B2 phase can be obtained in the as-cast $\text{Al}_x\text{Co}_{2-x}\text{CrFeNi}$ ($x = 1.0-1.75$) alloys.

3.2 Annealed Microstructure at 800 °C

After being annealed at 800 °C for 30 days (alloys A'1-A'7), both the phase constituents and microstructures greatly changed. Their XRD patterns and BSE images are presented in Fig. 3 and 4, respectively. The alloy

Table 1 Detected chemical compositions of arc-melted $Al_xCo_{2-x}CrFeNi$ ($x = 0.25-1.75$) alloys in the as-cast state and after annealing at 800 and 1000 °C for 30 days

Designed composition	No.	States	Phase/Region	Detected composition, at.%				
				Al	Co	Cr	Fe	Ni
5Al35Co20Fe20Cr20Ni ($x = 0.25$)	A1	As-cast	Total/FCC	5.1	34.5	20.2	20.1	20.1
	A'1	800 °C annealed	FCC	4.6	35.4	19.2	20.4	20.4
	A''1	1000 °C annealed	FCC	4.7	35.6	19.8	20.2	19.7
10Al30Co20Fe20Cr20Ni ($x = 0.5$)	A2	As-cast	Total	10.3	29.4	20.0	20.2	20.1
			FCC	9.1	30.1	21.5	20.5	18.8
			B2	25.5	22.6	13.3	12.5	26.1
	A'2	800 °C annealed	FCC + B2	8.4	30.5	20.3	20.7	20.1
			B2	31.6	18.2	5.5	10.1	34.6
	A''2	1000 °C annealed	FCC	6.6	31.5	22.1	21.3	18.5
B2			29.2	21.4	7.4	11.2	30.8	
15Al25Co20Fe20Cr20Ni ($x = 0.75$)	A3	As-cast	Total	15.4	24.8	19.9	19.9	20.0
			FCC	10.2	26.4	21.0	22.0	20.4
			B2	19.5	22.8	19.8	18.2	19.7
	A'3	800 °C annealed	FCC	8.5	22.6	23.9	28.4	16.6
			B2	27.8	19.8	10.6	13.1	28.7
			BCC	4.3	23.0	42.6	19.9	10.2
	A''3	1000 °C annealed	σ	Not detected. ^a				
			FCC	7.7	27.4	25.2	23.7	16.0
			B2	26.9	21.3	11.4	13.8	26.6
20Al20Co20Fe20Cr20Ni ($x = 1.0$)	A4	As-cast	Total/B2	19.3	20.0	20.3	20.3	20.1
			FCC	6.5	25.8	24.8	27.8	15.1
	A'4	800 °C annealed	B2	29.1	18.7	9.9	14.1	28.2
			BCC	5.9	19.8	40.8	24.2	9.3
			σ	Not detected. ^a				
	A''4	1000 °C annealed	FCC	6.0	23.5	27.7	28.0	14.8
B2			30.5	19.1	7.3	11.6	31.5	
25Al15Co20Fe20Cr20Ni ($x = 1.25$)	A5	As-cast	Total/B2	24.2	14.9	19.4	20.1	21.4
			B2	29.1	15.9	13.6	16.2	25.2
	A'5	800 °C annealed	BCC	15.8	14.6	30.4	24.4	14.8
			A''5	1000 °C annealed	B2	30.5	19.1	7.3
30Al10Co20Fe20Cr20Ni ($x = 1.5$)	A6	As-cast	BCC	6.8	13.9	42.3	30.2	6.8
			Total/B2	27.5	10.3	20.5	20.7	21.0
	A'6	800 °C annealed	BCC + B2 ^b	27.3	9.9	21.5	21.5	19.8
			A''6	1000 °C annealed	B2	38.7	12.5	5.8
	35Al5Co20Fe20Cr20Ni ($x = 1.75$)	A7	As-cast	BCC	9.2	6.6	44.9	34.6
Total/B2				33.9	5.3	20.1	20.1	20.6
A'7		800 °C annealed	BCC + B2 ^b	38.7	3.6	14.5	19.6	23.6
	A''7		1000 °C annealed	B2	42.9	6.9	6.9	12.7
			BCC/B2	19.2	2.7	40.2	31.1	6.8

^aThe σ phase is clearly identified by XRD. But its phase composition is not detected for the small phase size and limited color difference

^bThis is the average composition of a BCC + B2 region, because the phase size is too small to distinguish BCC and B2

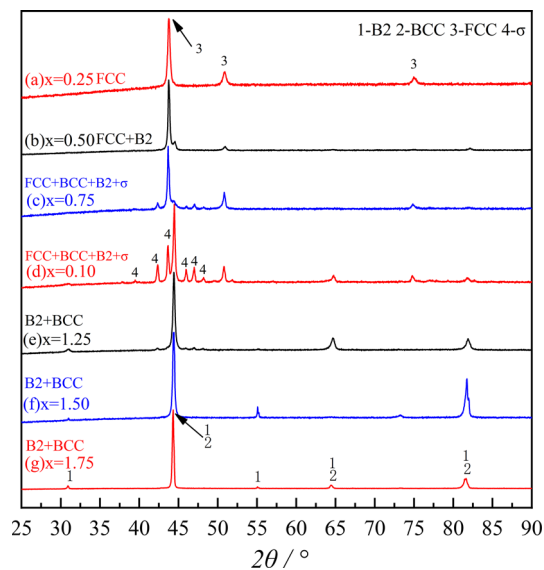
compositions and phase compositions detected by SEM-EDS are also listed in Table 1.

A small amount of the darker phase can be observed in alloy A'1. Compared to the as-cast alloys, this phase is

separated from the FCC phase during annealing at 800 °C. The phase is too small to be well detected by both XRD and SEM-EDS. It is believed that the darker grains are the ordered BCC (B2) phase, because it is much darker than

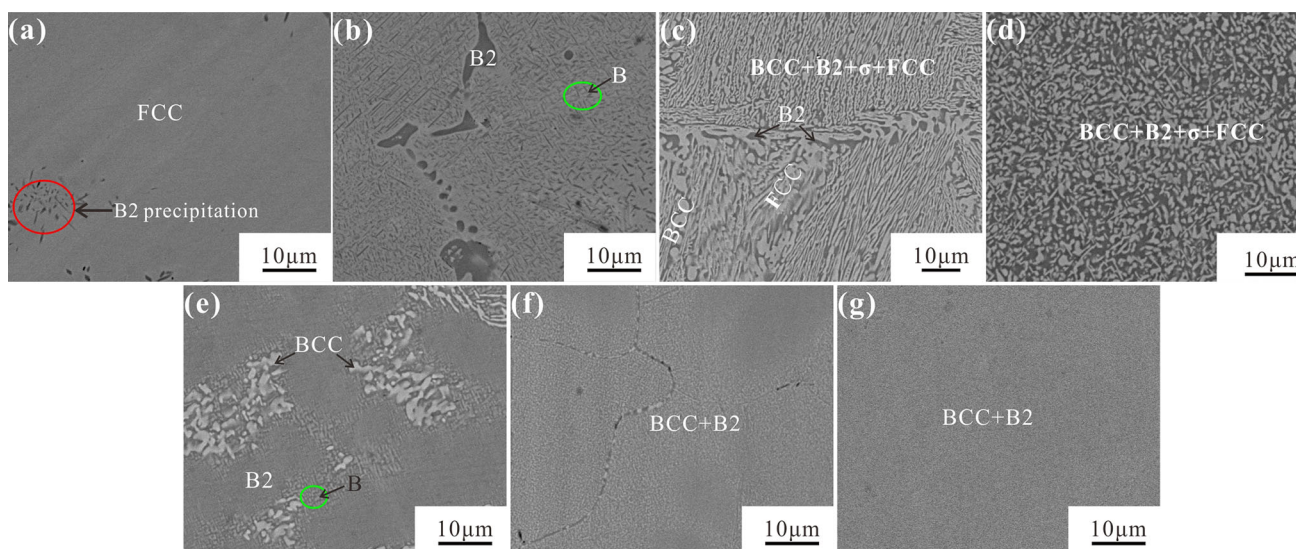
Table 2 Summarizing the composition range of the detected phases in the present work

Phases	Detected composition range, at.%				
	Al	Co	Cr	Fe	Ni
FCC	< 9.1	23.5-35.4	19.2-27.7	20.1-28.4	14.8-20.4
BCC	4.3-9.2	6.6-19.8	40.8-44.9	19.9-34.6	4.7-10.2
B2	25.5-42.9	6.9-22.8	5.5-13.6	10.1-16.2	25.2-31.5

**Fig. 3** XRD patterns of $\text{Al}_x\text{Co}_{2-x}\text{CrFeNi}$ alloys annealed at 800 °C for 30 days

FCC, which means much higher Al content. Since the Al content is up to 10 at.% (alloy B'2), the darker regions grow and the lighter areas appear as amplitude modulating decomposition (marked as “B”), which can promote the separation of the over-saturated components. EDS results show that the B2 phase is rich in Al and Ni and poor in Cr and Fe, while the FCC phase is a Co- and Fe-rich and Al-poor region. According to the EDS results in Table 1, the Al content of the FCC phase in the 800 °C annealed state is marginally lower than the as-cast state, i.e., the as-cast FCC phase is over-saturated with Al content.

As for the 800 °C annealed alloy A'3, its XRD pattern in Fig. 3(c) indicates that the major FCC phase and a small amount of the BCC-type and σ phases coexist. Compared to the as-cast alloy A3 (Fig. 1c), the characteristic peaks of the σ phase can be observed, i.e., the σ phase forms during annealing at 800 °C. However, we failed to distinguish its phase composition because these phases are too fine and have similar colours with other phases. The FCC and BCC phases also have no colour difference, but they can be distinguished by SEM–EDS. EDS results prove that some of the lighter grains are Cr-rich and Al-poor BCC phase, while some of them are FCC phase, which has much lower Cr content but with higher Fe and Ni content. Their composition are presented in Table 1. Moreover, the B2 phase can be identified by its colour and chemical composition, but not by XRD pattern for its limited volume fraction. The Al content in the darker B2 phase turns to be 27.8 at.% after 800 °C annealing, which is much higher than that of the as-cast B2 phase.

**Fig. 4** BSE micrographs of $\text{Al}_x\text{Co}_{2-x}\text{CrFeNi}$ alloys annealed at 800 °C for 30 days: (a) A'1, $x = 0.25$; (b) A'2, $x = 0.50$; (c) A'3, $x = 0.75$; (d) A'4, $x = 1.00$; (e) A'5, $x = 1.25$; (f) A'6, $x = 1.50$; (g) A'7, $x = 1.75$

The 800 °C annealed alloy A'4 alloy (20Al20Co20-Fe20Cr20Ni) also contains the B2, BCC, FCC and σ phases. The characteristic peaks of the σ , FCC, and B2 phases can be well indexed in its XRD patterns (Fig. 3d). From Fig. 3(d), it seems that the alloys should have a distinct volume fraction of the σ phase, but the grains are too small to examine its composition. Actually, the similar structure was also reported by Lim et al.,^[37] in which the AlCoCrFeNi alloy was heat-treated at 700 °C for 6 h and had smaller grain size. They pointed out that the dendritic region had BCC-A2 and BCC-B2 dual-phase structure. As for the alloy A'5, its XRD pattern shows that the major phase in the alloys is B2, just small amount of σ phase exist, while the FCC phase is totally disappeared.

Both alloys A'6 and A'7 include the BCC and B2 phases. Although the characteristic peaks of BCC phase are overlapped by B2 phase, two phases can be distinguished in their BSE image, as shown in Fig. 4(f) and (g). These two phases are too fine to be detected their compositions by EDS. That is to say, the BCC phase will precipitate from the as-cast B2 phase in $\text{Al}_x\text{Co}_{2-x}\text{CrFeNi}$ ($x = 1.5\text{--}0.175$) alloys. As can be seen from Fig. 4(f) and (g), the phase size in alloy A'7, with higher Al content, is finer than that in alloy A'6.

3.3 Annealed Microstructure at 1000 °C

The microstructure of the alloys changes obviously and the over-saturated solid solution tends to stabilise after being annealed at 1000 °C for 30 days. Their XRD patterns and SEM images are presented in Fig. 5 and 6, respectively.

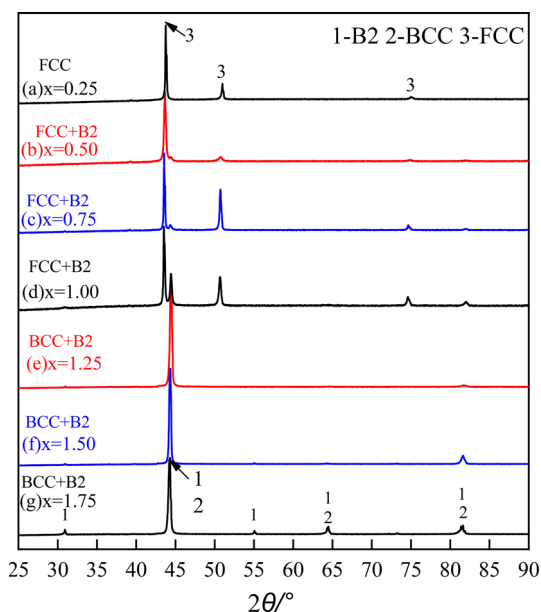


Fig. 5 XRD patterns of $\text{Al}_x\text{Co}_{2-x}\text{CrFeNi}$ alloys annealed at 1000 °C for 30 days

The EDS results are also included in Table 1. Compared to the 800 °C annealing for 30 days, the grains become coarser and the σ -FeCr phase disappears.

As can be seen from Fig. 5(a) and 6(a), the alloy A''1 still contains the single FCC phase. The alloy A''2 contains two different regions and the needle- and plate-like B2 phase precipitated from the FCC phase. The EDS results reveal that the B2 phase is rich in Al and Ni while the FCC phase is rich in Co and Fe. XRD patterns can identify these two phases apparently, but the volume fraction of B2 phase in alloy A''2 is limited. With the Al content increasing to 15–20%, the microstructure turns into dendritic. The dendrites contain the FCC phase and the interdendritic includes the B2 phase. The amount of B2 phase increases gradually from alloy A''1 to A''4. And the FCC phase disappears when the Al content reaches 20% (alloy A''5). As shown in Fig. 6(e–g), it is clear that alloys A''5–7 contain two phases. Based on EDS results and XRD patterns, they are confirmed to be BCC + B2 phases. The existence of small peaks at 30.9° (2θ) indicates that these alloys contain B2 phase. Compared with the as-cast microstructure, the Cr-rich BCC phase, with the composition of 6.8Al–13.9Co–42.3Cr–30.2Fe–6.8Ni, forms after annealing. With further increasing of the Al content, the size of the BCC phase decreases from 1.6 to 1.0 μm in alloys A''6 and A''7, respectively.

3.4 Microhardness of $\text{Al}_x\text{Co}_{2-x}\text{CrFeNi}$ Alloys

Figure 7 shows the microhardness of the $\text{Al}_x\text{Co}_{2-x}\text{CrFeNi}$ alloys in the as-cast or 800 and 1000 °C annealed states. With the exception of alloy A5 in the as-cast and 800 °C annealed states, the hardness of alloys tends to increase with Al content.

With fixed Cr, Fe and Ni contents at 20%, the hardness of the as-cast $\text{Al}_x\text{Co}_{2-x}\text{CrFeNi}$ ($x = 0.25\text{--}1.75$) alloys changes from 138 HV (A1) to 603 HV (A7) with the increase of the Al content. After being annealed at 800 °C for 30 days, their hardness decreases from 167 HV (A'1) to 556 HV (A'4). For the eutectic structure existed in alloy A3, its hardness even increases after 800 °C annealing. Moreover, the hardness of alloys dramatically decreases after 1000 °C annealing. This is because the grains become coarser. The largest change of hardness is the equiatomic AlCoCrFeNi (A''4) alloy because of the coarse FCC grains forming. The maximum difference values of the as-cast alloys that exceed the 800 and 1000 °C annealed states alloys are 55 and 143 HV, respectively.

The BCC-type and σ phases can harden the alloys while the FCC phase can soften them. Therefore, the tendency of hardness increases with Al content. The hardness of alloy A'4 is larger than that of alloy A'5 at 800 °C, because the lower amount of the σ phase. In addition, it has been

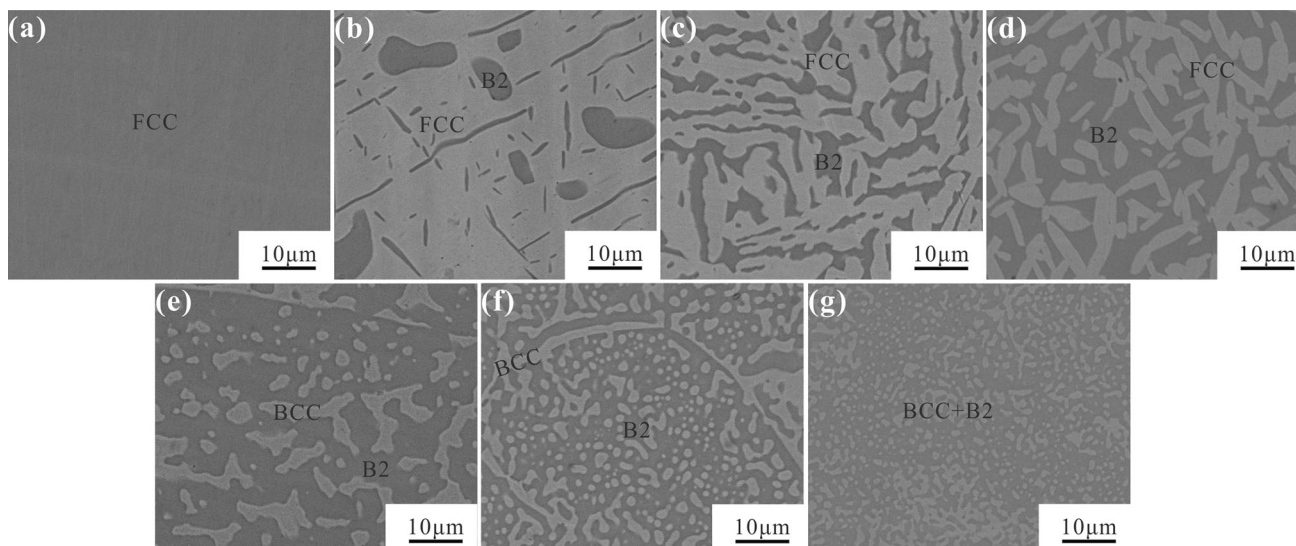


Fig. 6 BSE micrographs of $\text{Al}_x\text{Co}_{2-x}\text{CrFeNi}$ alloys annealed at 1000 °C for 30 days: (a) A''1, $x = 0.25$; (b) A''2, $x = 0.50$; (c) A''3, $x = 0.75$; (d) A''4, $x = 1.00$; (e) A''5, $x = 1.25$; (f) A''6, $x = 1.50$; (g) A''7, $x = 1.75$

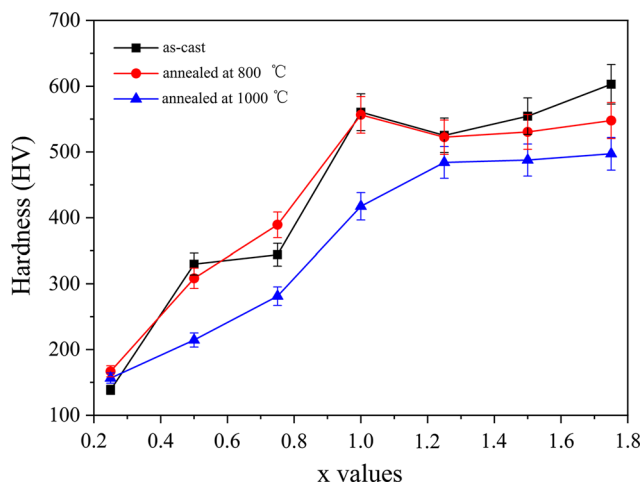


Fig. 7 Microhardness of $\text{Al}_x\text{Co}_{2-x}\text{CrFeNi}$ ($x = 0.25$ -1.75) alloys

proved that the mismatch between the BCC and B2 phases, which form intervened structures containing many interfaces with coherent internal stresses, can contribute to a certain amount of hardening.^[38] The smaller width would possess a higher interfacial area and thus a high hardness value.^[16] The grain size of alloys A5-A7 becomes smaller (Fig. 4e–g and 6e–g), which leads to the slight rise in hardness from alloys A5-A7 annealed at 800 and 1000 °C for 30 days.

4 Discussion

As discussed above, the microstructure of the $\text{Al}_x\text{Co}_{2-x}\text{CrFeNi}$ ($x = 0.25$ -1.75) alloys transforms obviously by adjusting the Al and Co content or changing the annealing

temperature. With the increase of the Al content, the phase composition of the $\text{Al}_x\text{Co}_{2-x}\text{CrFeNi}$ alloys transforms from FCC to FCC + B2 and then to the BCC-type phases. According to the EDS results in Table 1, less than 9.1 at.% Al and more than 23.5 at.%Co was detected in the annealed FCC phase; the BCC phase is enriched in Cr content (> 40.8 at.%) and low Al content; while the Al content in the B2 phase is above 25% in annealed alloys. It needs to note that the composition of the BCC phase in 800 °C annealed alloy A'5 may not accurate enough for its small size. The composition ranges of the FCC, BCC and B2 phases detected in the present work are summarized in Table 2.

The microstructure changes obviously and new phases separate out after annealing. After being annealed at 800 °C for 30 days, both alloys A'2 ($\text{Al}_{0.5}\text{Co}_{1.5}\text{CrFeNi}$) and A'5 ($\text{Al}_{1.25}\text{Co}_{0.75}\text{CrFeNi}$) display amplitude modulating decomposition, which is beneficial for separating the over-saturated elements. Alloys A'3 ($\text{Al}_{0.75}\text{Co}_{1.25}\text{CrFeNi}$) and A'4 (AlCoCrFeNi) show a dendritic structure while alloys A'6 ($\text{Al}_{1.5}\text{Co}_{0.5}\text{CrFeNi}$) and A'7 ($\text{Al}_{1.75}\text{Co}_{0.25}\text{CrFeNi}$) are uniform. Although the alloys were annealed at 800 °C for 30 days, the grain size is still very small. Anyway, the σ phase can make the alloy hard and brittle.^[39] But it is unstable at 1000 °C in these alloys. Compared to 800 °C annealed alloys, the grain size in the 1000 °C annealed alloys becomes much larger. These results have the same tendency by Wang et al.^[22] for the $\text{Al}_x\text{CoCrFeNi}$ alloys. Therefore, the Al content is the key factor that determines the amount of the BCC phase. In addition, as has been proved, the B2 phase can strengthen the BCC phase to harden the alloys.^[40] From the SEM images of Fig. 4 and 6, the volume fraction of the B2 phase

at 1000 °C is different from that of 800 °C annealed alloys with the same composition. Moreover, upon increasing the annealing temperature to 1000 °C, the grain size become much larger, which leads a decrease in the alloy hardness. In addition, except for alloy A[#]1 (Al_{0.25}Co_{1.75}CrFeNi, Fig. 6a), the phase boundary in the 1000 °C annealed alloys can be observed distinctly.

5 Conclusions

The phase constituent, microstructure and microhardness of the Al_xCo_{2-x}CrFeNi alloys in as-cast and 800 or 1000 °C annealed states were investigated in the present work. After being annealed for 30 days, the phases tended to stabilise and the microstructure and hardness of the alloys changed transparently. Based on the experimental results and analysis, the following conclusions can be drawn:

1. With the increase of the Al content, the phases in the as-cast Al_xCo_{2-x}CrFeNi ($x = 0.25-1.75$) alloys change from FCC to FCC + B2 and then to B2.
2. The eutectic structure exists in the as-cast and 800 °C annealed Al_{0.75}Co_{1.25}CrFeNi alloy. After annealing at 1000 °C, it turns to the coarse grains of the FCC and B2 phases.
3. The single B2 phase can be obtained in the as-cast Al_xCo_{2-x}CrFeNi ($x = 1-1.75$) alloys. After annealing at 800-1000 °C, the BCC phase will precipitate from the B2 phase in these alloys.
4. The σ phase forms in the 800 °C annealed Al_xCo_{2-x}CrFeNi ($x = 0.75-1.25$) alloys. However, it cannot exist in the 1000 °C annealed alloys.
5. The hardness of as-cast alloys can reach 603 HV. The annealed samples at 800 and 1000 °C can achieve 556 and 497 HV, respectively.

Acknowledgments The authors gratefully acknowledge the financial support from National Natural Science Foundation of China (Nos. 51771035 and 51671036), Natural Science Foundation of Jiangsu Province (BK20161190), Postgraduate Research and Practice Innovation Program of School of Materials Science and Engineering Changzhou University (CL17SJ-003) and the Priority Academic Program Development of Jiangsu Higher Education Institutions.

References

1. Y. Zhang, T.T. Zuo, Z. Tang, M.C. Gao, K.A. Dahmen, P.K. Liaw, and Z.P. Lu, Microstructures and Properties of High-Entropy Alloys, *Prog. Mater. Sci.*, 2014, **61**, p 1-93
2. D.B. Miracle and O.N. Senkov, A Critical Review of High Entropy Alloys and Related Concepts, *Acta Mater.*, 2017, **122**, p 448-511
3. B. Cantor, I.T.H. Chang, P. Knight, and A.J.B. Vincent, Microstructural Development in Equiatomic Multicomponent Alloys, *Mater. Sci. Eng. A*, 2004, **375-377**, p 213-218
4. J.W. Yeh, S.K. Chen, S.J. Lin, J.Y. Gan, T.S. Chin, T.T. Shun, C.H. Tsau, and S.Y. Chang, Nanostructured High-Entropy Alloys with Multiple Principal Elements: Novel Alloy Design Concepts and Outcomes, *Adv. Eng. Mater.*, 2004, **6**(5), p 299-303
5. F. He, Z. Wang, Q. Wu, S. Niu, J. Li, J. Wang, and C.T. Liu, Solid Solution Island of the Co-Cr-Fe-Ni High Entropy Alloy System, *Scr. Mater.*, 2017, **131**, p 42-46
6. B. Gludovatz, A. Hohenwarter, D. Catoor, E.H. Chang, E.P. George, and R.O. Ritchie, A Fracture-Resistant High-Entropy Alloy for Cryogenic Applications, *Science*, 2014, **345**(6201), p 1153-1158
7. K.B. Zhang, Z.Y. Fu, J.Y. Zhang, W.M. Wang, S.W. Lee, and K. Niihara, Annealing Effects on Structure and Mechanical Properties of CoCrFeNiTiAl_x High-Entropy Alloys, *IOP Conf. Ser. Mater. Sci. Eng.*, 2011, **20**, p 012009
8. J.Y. He, W.H. Liu, H. Wang, Y. Wu, X.J. Liu, T.G. Nieh, and Z.P. Lu, Effects of Al Addition on Structural Evolution and Tensile Properties of the FeCoNiCrMn High-Entropy Alloy System, *Acta Mater.*, 2014, **62**, p 105-113
9. P. Yang, Y. Liu, X. Zhao, J. Cheng, and H. Li, Electromagnetic Wave Absorption Properties of FeCoNiCrAl_{0.8} High Entropy Alloy Powders and Its Amorphous Structure Prepared by High-Energy Ball Milling, *J. Mater. Res.*, 2016, **31**(16), p 2398-2406
10. W.H. Liu, J.Y. He, H.L. Huang, H. Wang, Z.P. Lu, and C.T. Liu, Effects of Nb Additions on the Microstructure and Mechanical Property of CoCrFeNi High-Entropy Alloys, *Intermetallics*, 2015, **60**, p 1-8
11. A.S.M. Ang, C.C. Berndt, M.L. Sesso, A. Anupam, S. Praveen, R.S. Kottada, and B.S. Murty, Plasma-Sprayed High Entropy Alloys: Microstructure and Properties of AlCoCrFeNi and MnCoCrFeNi, *Metall. Mater. Trans. A*, 2015, **46**(2), p 791-800
12. S. Antonov, M. Detrois, and S. Tin, Design of Novel Precipitate-Strengthened Al-Co-Cr-Fe-Nb-Ni High-Entropy Superalloys, *Metall. Mater. Trans. A*, 2018, **49**(1), p 305-320
13. J.W. Qiao, S.G. Ma, E.W. Huang, C.P. Chuang, P.K. Liaw, and Y. Zhang, Microstructural Characteristics and Mechanical Behaviors of AlCoCrFeNi High-Entropy Alloys at Ambient and Cryogenic Temperatures, *Mater. Sci. Forum*, 2011, **688**, p 419-425
14. H.-P. Chou, Y.-S. Chang, S.-K. Chen, and J.-W. Yeh, Microstructure, Thermophysical and Electrical Properties in Al_xCoCrFeNi ($0 \leq x \leq 2$) High-Entropy Alloys, *Mater. Sci. Eng. B*, 2009, **163**(3), p 184-189
15. C.-M. Lin and H.-L. Tsai, Evolution of Microstructure, Hardness, and Corrosion Properties of High-Entropy Al_{0.5}CoCrFeNi Alloy, *Intermetallics*, 2011, **19**(3), p 288-294
16. W.-R. Wang, W.-L. Wang, S.-C. Wang, Y.-C. Tsai, C.-H. Lai, and J.-W. Yeh, Effects of Al Addition on the Microstructure and Mechanical Property of Al_xCoCrFeNi High-Entropy Alloys, *Intermetallics*, 2012, **26**, p 44-51
17. N. Park, I. Watanabe, D. Terada, Y. Yokoyama, P.K. Liaw, and N. Tsuji, Recrystallization Behavior of CoCrCuFeNi High-Entropy Alloy, *Metall. Mater. Trans. A*, 2015, **46**(4), p 1481-1487
18. T.M. Butler and M.L. Weaver, Oxidation Behavior of Arc Melted AlCoCrFeNi Multi-Component High-Entropy Alloys, *J. Alloys Compd.*, 2016, **674**, p 229-244
19. G. Liu, L. Liu, X. Liu, Z. Wang, Z. Han, G. Zhang, and A. Kostka, Microstructure and Mechanical Properties of Al_{0.7}CoCrFeNi High-Entropy-Alloy Prepared by Directional Solidification, *Intermetallics*, 2018, **93**, p 93-100
20. G. Qin, W. Xue, C. Fan, R. Chen, L. Wang, Y. Su, H. Ding, and J. Guo, Effect of Co Content on Phase Formation and Mechanical

- Properties of (AlCoCrFeNi)_{100-x}Cox High-Entropy Alloys, *Mater. Sci. Eng. A*, 2018, **710**, p 200-205
21. J.C. Rao, V. Ocelik, D. Vainchtein, Z. Tang, P.K. Liaw, and J.T.M. De Hosson, The FCC-BCC Crystallographic Orientation Relationship in Al_xCoCrFeNi High-Entropy Alloys, *Mater. Lett.*, 2016, **176**, p 29-32
 22. W.-R. Wang, W.-L. Wang, and J.-W. Yeh, Phases, Microstructure and Mechanical Properties of Al_xCoCrFeNi High-Entropy Alloys at Elevated Temperatures, *J. Alloys Compd.*, 2014, **589**, p 143-152
 23. P.F. Yu, H. Cheng, L.J. Zhang, H. Zhang, Q. Jing, M.Z. Ma, P.K. Liaw, G. Li, and R.P. Liu, Effects of High Pressure Torsion on Microstructures and Properties of an Al_{0.1}CoCrFeNi High-Entropy Alloy, *Mater. Sci. Eng. A*, 2016, **655**, p 283-291
 24. T. Yang, S. Xia, S. Liu, C. Wang, S. Liu, Y. Zhang, J. Xue, S. Yanand, and Y. Wang, Effects of AL Addition on Microstructure and Mechanical Properties of Al_xCoCrFeNi High-Entropy Alloy, *Mater. Sci. Eng. A*, 2015, **648**, p 15-22
 25. Q. Chao, T. Guo, T. Jarvis, X. Wu, P. Hodgson, and D. Fabijanic, Direct Laser Deposition Cladding of Al_xCoCrFeNi High Entropy Alloys on a High-Temperature Stainless Steel, *Surf. Coat. Technol.*, 2017, **332**, p 440-451
 26. C. Li, J.C. Li, M. Zhao, and Q. Jiang, Effect of Aluminum Contents on Microstructure and Properties of Al_xCoCrFeNi Alloys, *J. Alloys Compd.*, 2010, **504**, p S515-S518
 27. Y. Shi, L. Collins, R. Feng, C. Zhang, N. Balke, P.K. Liaw, and B. Yang, Homogenization of Al_xCoCrFeNi High-Entropy Alloys with Improved Corrosion Resistance, *Corros. Sci.*, 2018, **133**, p 120-131
 28. J.C. Rao, H.Y. Diao, V. Ocelik, D. Vainchtein, C. Zhang, C. Kuo, Z. Tang, W. Guo, J.D. Poplawsky, Y. Zhou, P.K. Liaw, and J.T.M. De Hosson, Secondary Phases in Al_xCoCrFeNi High-Entropy Alloys: An In Situ TEM Heating Study And Thermodynamic Appraisal, *Acta Mater.*, 2017, **131**, p 206-220
 29. T. Yang, S. Xia, S. Liu, C. Wang, S. Liu, Y. Fang, Y. Zhang, J. Xue, S. Yanand, and Y. Wang, Precipitation Behavior of Al(x)-CoCrFeNi High Entropy Alloys Under Ion Irradiation, *Sci. Rep.*, 2016, **6**, p 32146
 30. A. Munitz, L. Meshi, and M.J. Kaufman, Heat Treatments' Effects on the Microstructure and Mechanical Properties of an Equiatomic Al-Cr-Fe-Mn-Ni High Entropy Alloy, *Mater. Sci. Eng. A*, 2017, **689**, p 384-394
 31. D. Li, C. Li, T. Feng, Y. Zhang, G. Sha, J.J. Lewandowski, P.K. Liaw, and Y. Zhang, High-Entropy Al_{0.3}CoCrFeNi Alloy Fibers with High Tensile Strength and Ductility at Ambient and Cryogenic Temperatures, *Acta Mater.*, 2017, **123**, p 285-294
 32. S. Niu, H. Kou, T. Guo, Y. Zhang, J. Wang, and J. Li, Strengthening of Nanoprecipitations in an Annealed Al_{0.5}CoCrFeNi High Entropy Alloy, *Mater. Sci. Eng. A*, 2016, **671**, p 82-86
 33. T.M. Butler and M.L. Weaver, Investigation of the Phase Stabilities in AlNiCoCrFe High Entropy Alloys, *J. Alloys Compd.*, 2017, **691**, p 119-129
 34. C.W. Tsai, M.H. Tsai, K.Y. Tsai, S.Y. Chang, J.W. Yeh, and A.C. Yeh, Microstructure and Tensile Properties of Al_{0.5}CoCrCuFeNi Alloys Produced by Simple Rolling and Annealing, *Mater. Sci. Technol.*, 2015, **31**(10), p 1178-1183
 35. X. Wu, W. Zhang, L. Qin, and C. Zhang, Effects of Annealing Treatment on Microstructure and Mechanical Properties of AlCoCrFeNi High-entropy Alloy, *Hot Work. Technol.*, 2015, **44**(8), p 220-222
 36. C. Wu, Y. Sun, Y. Liu, and H. Tu, Effect of Long-Time Annealing at 1000 °C on Phase Constituent and Microhardness of the 20Co-Cr-Fe-Ni Alloys, *Materials*, 2019, **12**(10), p 1700
 37. K.R. Lim, K.S. Lee, J.S. Lee, J.Y. Kim, H.J. Chang, and Y.S. Na, Dual-Phase High-Entropy Alloys for High-Temperature Structural Applications, *J. Alloys Compd.*, 2017, **728**, p 1235-1238
 38. M. Kato, Hardening by Spinodally Modulated Structure in BCC Alloys, *Acta Metall.*, 1981, **29**(1), p 79-87
 39. N.D. Stepanov, D.G. Shaysultanov, G.A. Salishchev, M.A. Tikhonovsky, E.E. Oleynik, A.S. Tortika, and O.N. Senkov, Effect of V Content on Microstructure and Mechanical Properties of the CoCrFeMnNiV_x High Entropy Alloys, *J. Alloys Compd.*, 2015, **628**, p 170-185
 40. C. Li, M. Zhao, J.C. Li, and Q. Jiang, B2 Structure of High-Entropy Alloys with Addition of Al, *J. Appl. Phys.*, 2008, **104**(11), p 113504
- Publisher's Note** Springer Nature remains neutral with regard to jurisdictional claims in published maps and institutional affiliations.